ACS APPLIED BIO MATERIALS

www.acsabm.org Article

First Lanthanide Complex for *De Novo* Phasing in Native Protein Crystallography at 1 Å Radiation

Alejandro Prieto-Castañeda, Siseth Martínez-Caballero, Antonia R. Agarrabeitia, Inmaculada García-Moreno, Santiago de la Moya, María J. Ortiz,* and Juan A. Hermoso*

Cite This: *ACS Appl. Bio Mater.* 2021, 4, 4575–4581 Read Online

ACCESS | Metrics & More | Article Recommendations

ABSTRACT: Phasing agents enabling *de novo* protein structure determination at *ca.* 1 Å, the wavelength corresponding to the maximum intensity of the synchrotron facilities applied in biomacromolecular crystallography, have been long sought-after. The first phasing agent designed for solving native protein structures at 0.97934 Å is described herein. The agent consists of a neutral ytterbium(III)-caged complex that exhibits higher anomalous signals at shorter wavelengths when compared to the best, currently applied lanthanide-based phasing agents, all of them based on gadolinium or terbium. As a proof of principle, the complex allows determining the 3D structure of a 36 kDa protein without setting the incident beam wavelength at the metal absorption edge, the strategy followed to date to gain the strongest anomalous signal even at the expense of crystallographic resolution. The agent becomes nondisruptive to the diffraction quality of the marked crystals and allows determining accurate phases, both leading to high-quality electron-density maps that enable the full tracing of the protein structure only with one agent unit bound to the protein. The high phasing power, efficient binding to the protein, low metal−macromolecule ratio, and easy handling support the developed Yb(III) complex as the best phasing agent for X-ray crystallography of a complex biomacromolecule without using modified analogues.

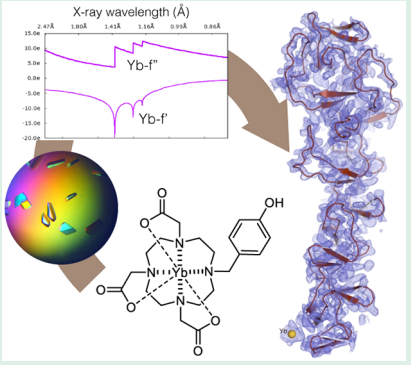

KEYWORDS: *lanthanide(III)-caged complex, X-ray crystallography, protein crystallography, SAD phasing, metals*

INTRODUCTION

Nowadays, X-ray crystallography is the most successful technique for determining the 3D structure of proteins and other biomacromolecules, which is essential for advances in biomedicine. Unfortunately, the well-known "phase problem" used to be a limitation for such structural determination. In the absence of homologous structures capable of providing the phases by the molecular replacement method, experimental phases remain essential. Decorating the crystals with heavy atoms capable of producing anomalous diffraction is a useful strategy to solve this problem, which is currently done by the well-established single- or multiple-wavelength anomalous diffraction (SAD or MAD, respectively) techniques.[1,2] In the case of protein crystals, such a heavy-atom decoration can be conducted by different ways (e.g., by biologically producing protein analogues in which methionines are substituted by "heavy" selenomethionines[3,4]). Nonetheless, treating the crystals (by co-crystallization or soaking) with an exogenous heavy-atom derivatizing agent (the phasing agent) is an interesting alternative to the preparation of protein analogues involving "heavy" amino acids. However, the most popular phasing agents used for this valuable purpose (e.g., gold,[5] bromine, iodine,[6−10] certain metallic salts,[11−13] polymetallic clusters,[14,15] or heavy noble gases[16]) present important drawbacks, mainly related with the lack of generality when applied to different protein crystals, low solubility in the mother liquor in which the protein crystallizes or is soaked, low intrinsic efficiency for producing the required anomalous signalization, and/or low efficiency for a proper heavy-atom derivatization (e.g., low ratio of structure-distorting heavy atoms per macromolecule unit).[17]

Certain heavy metal complexes have also been used as successful phasing agents to resolve the structure of protein crystals[18−27] and complex, large molecular assemblies by the SAD technique.[28] The anomalous phasing power of these agents is proportional to the imaginary part of the atomic scattering factor, f'', of the involved heavy atom and to the occupancy of its binding site, the latter influencing the effectiveness of the bound protein. Lanthanide (Ln) atoms provide high anomalous scattering, due to a white line, with f'' ∼ 28 e^-, in their L_{III} absorption edge. In this context, a new

Received: March 12, 2021
Accepted: April 16, 2021
Published: April 29, 2021

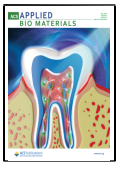

https://doi.org/10.1021/acsabm.1c00305
ACS Appl. Bio Mater. 2021, 4, 4575–4581

Scheme 1. Synthesis of Phasing Agent 1: (i) K_2CO_3, CH_3CN, 55 °C, 3.5 h; (ii) aq NaOH 3 M, aq H_2O_2 10 M, THF, rt, 4 h; (iii) TFA, rt, 12 h; (iv) $YbCl_3 \cdot 6H_2O$, H_2O, pH 6.5, rt, 3.5 h

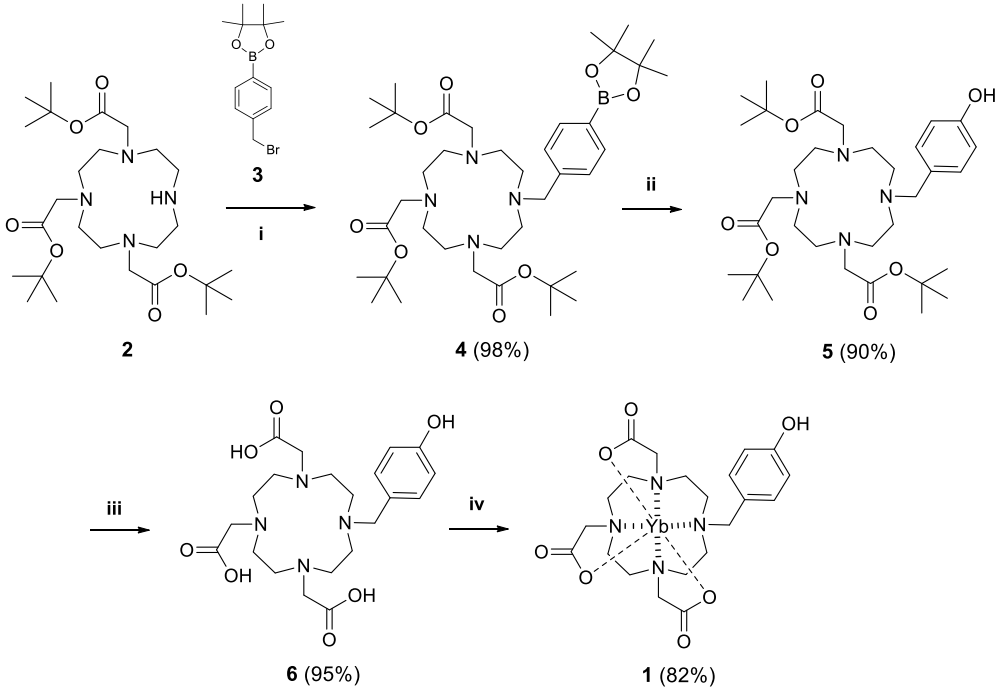

class of phasing agents based on Gd(III) clathrochelate (*i.e.*, a metal cage complex) has been reported to be a successful tool for obtaining heavy-atom-decorated protein crystals that are suitable for experimental phasing by using the strong anomalous signal at the Gd L_{III} absorption edge ($f'' = 28$ e^-, $\lambda = 1.711$ Å).[29−38] Interestingly, even at Cu Kα radiation ($\lambda = 1.5418$ Å), the wavelength regularly used in in-house rotating anode devices, such gadolinium-decorated crystals yield a high anomalous signal ($f'' = 12$ e^-), even higher than the anomalous signal obtained from Se at the K absorption edge ($f'' = 6-10$ e^-).

The Gd(III)-caged complexes have been used to phase some model proteins,[28,39,40] and to solve new macromolecular structures,[36] as well as to *de novo* phasing by serial femtosecond crystallography.[41] However, these complexes, while being powerful and versatile phasing agents, have the inconvenience of exhibiting the maximum anomalous signal at a long wavelength ($\lambda = 1.7118$ Å), far from the wavelengths typically used in biomacromolecular X-ray crystallography (around 1 Å) at synchrotron radiation facilities and for which most of the synchrotron beamlines are not optimized. Thus, it is well known that beamlines working at non-optimized longer wavelengths usually limit both the maximum resolution and the data quality through increased absorption, radiation damage, and harmonic contamination probability.[42] Besides, when data resolution is limited by the detector size, it may be advantageous to work at a shorter wavelength. Trying to overcome these shortcomings and fit the wavelength of lanthanide L_{III} absorption edge to those supplied by the X-ray radiation facilities, recently, a terbium-caged complex has been developed as a new phasing agent. However, its phasing properties were evaluated only by performing anomalous-based experiments at the Tb L_{III} absorption edge ($\lambda = 1.6500$ Å), that is, by setting the incident beam energy to optimally exploit the f'' contribution.[43]

Despite this active research work, smarter phasing agents based on Ln(III)-caged complex enabling *de novo* structure determination at *ca.* 1 Å of nonmodified (native) proteins are still much sought-after. A rational molecular design by selecting properly both the involved metallic center and the surrounding organic clathrochelating ligand could lead to advanced phasing agents, opening the viability for modulating stability, heavy-atom-decorating efficiency, phasing efficiency, and application scope. To explore this hypothesis, herein, we describe the design, synthetic development, and workability of a neutral Yb(III)-caged complex **1** (Scheme 1) endowed with both efficient decorating ability and efficient phasing power. As any lanthanide, ytterbium provides a strong anomalous signal ($f'' \sim 28e^-$) at its L_{III} absorption edge, the advantage with the related gadolinium or terbium complexes being the Yb L_{III} absorption edge taking place at $\lambda = 1.3863$ Å and thus closer to the wavelengths typically used in biomacromolecular crystallography beamlines, while keeping an excellent signal for in-house Cu Kα radiation.

EXPERIMENTAL SECTION

Materials and Methods. Anhydrous solvents were prepared by distillation over standard drying agents according to common methods. All other solvents were of HPLC-grade and were used as provided. Starting chemical substrates and reagents were used as commercially provided unless otherwise indicated. Tri-*tert*-butyl 1,4,7,10-tetraazacyclododecane-1,4,7-triacetate (**2**) (97%, Sigma-Aldrich) and 4-(bromomethyl)phenylboronic acid pinacol ester (**3**) (95% Alfa Aesar) were used as starting materials for the complex synthesized. High-resolution mass spectrometry (HRMS) was performed using matrix-assisted laser desorption ionization time-of-flight analysis.

Synthetic Procedure. The neutral Yb(III)-caged complex **1** was synthesized following the protocol depicted in Scheme 1. *N*-Alkylation of **2** with **3**, according to a previously described procedure,[44] efficiently yielded boronic ester **4**[45] (98% yield). After this, oxidative hydrolysis of boronate **4** under the described conditions

https://doi.org/10.1021/acsabm.1c00305
ACS Appl. Bio Mater. 2021, 4, 4575−4581

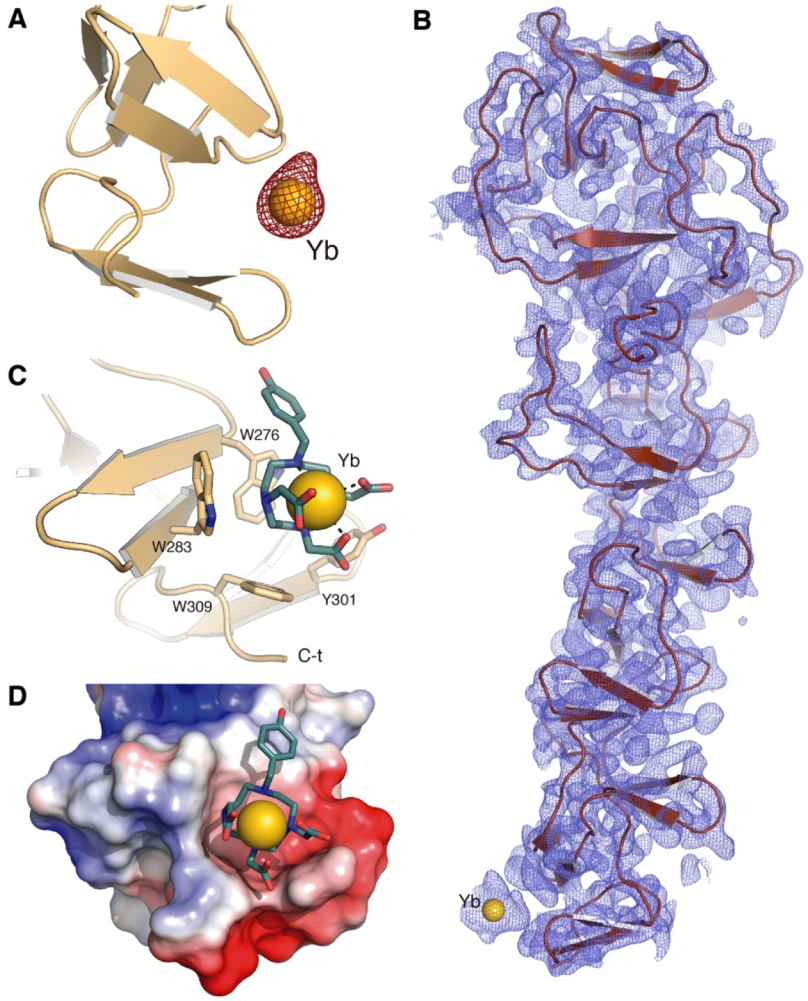

Figure 1. Phasing results and binding mode for: (A) anomalous difference map, contoured at 4σ, showing the position of the Yb atom. (B) 2Fo−Fc experimental map calculated with one Yb atom (drawn as yellow sphere) from the CbpF:**1** complex. The final 3D structure of CbpF (drawn as red cartoon) is superimposed for comparison purposes. Experimental map allowed full modeling of the complete CbpF structure. (C) Refined model of **1** (green sticks) bound to a choline-binding site of CbpF. Relevant residues are represented as capped sticks and labeled. (D) Electrostatic potential surface of CbpF colored from blue (electropositive) to red (electronegative). Refined model of **1** is represented as capped sticks, with the Yb atom as a yellow sphere.

yielded the corresponding phenol **5** (90% yield),[45] whose treatment with trifluoroacetic acid (TFA) afforded **6** (95% yield, as a trifluoroacetate salt).[45]

Synthesis of Cage Complex ***1****.* To a solution of **6** (40 mg, 0.088 mmol) in H_2O (1 mL) was slowly added Na_2CO_3 until the pH was adjusted to 6.5 and then a solution of $YbCl_3{\cdot}6H_2O$ (34.2 mg, 0.088 mmol) in H_2O (1 mL). The resulting mixture was stirred at room temperature (rt) for 3.5 h. After that, the pH was raised to 8.5 by adding 1 M NaOH, and the resulting basic solution was centrifuged at 5000 rpm for 60 min. The resulting supernatant liquid layer was removed, the solid layer was carefully washed with acetone, and dried under reduced pressure to afford **1** (45.2 mg, 82%) as a beige solid. HRMS m/z [M + H^+] 624.1491 (calcd for $C_{21}H_{30}N_4O_7Yb^+$, 624.1498).

Crystallization and X-ray Crystallography. Protein CbpF was expressed and purified as reported previously.[33] The protein was concentrated to 5 mg/mL, and the crystals were obtained by the sitting drop vapor diffusion technique, mixing 1 μL of protein and 1 μL of precipitant solution [0.2 M ammonium sulfate, 28% poly(ethylene glycol) (PEG) 8000, and 0.1 M sodium cacodylate buffer pH 6.5]. Derivative crystals were prepared by fast soaking (around 10 s) using the native crystallization conditions plus 25 mM of **1**. The crystals were cryoprotected in the precipitant solution supplemented with 30% glycerol and cooled at 100 K. Diffraction data sets were collected from the XALOC beamline at the ALBA synchrotron facility (Barcelona, Spain), using a Pilatus 6 M detector and a wavelength of 0.97934 Å. The collected data sets were processed with XDS[31] and Aimless.[30] The CbpF:**1** complex structure was solved by two methods: (i) the molecular replacement method as the control, using MOLREP[37] program and the CbpF native structure (PDB code 2V05) as the template and (ii) the SAD method. The heavy atom position, calculation of initial phases, construction, and refinement of the model were successfully obtained using CRANCK2[35] from CCP4 pack. The coordinates were refined using Phenix[46] and modeled using Coot.[29]

RESULTS AND DISCUSSION

Phasing Agent Design and Synthetic Development. For the design of a new lanthanide complex capable of efficiently acting as a smarter phasing agent for *de novo* protein structure determination, the following premises were taken into consideration: (1) selection of ytterbium, specifically Yb(III), as the metallic center to provide a high phasing power together with minimal crystal degradation due to absorption when using an X-ray wavelength of *ca.* 1 Å (specifically 0.97934 Å), the latter being optimal in synchrotron facilities devoted to

https://doi.org/10.1021/acsabm.1c00305
ACS Appl. Bio Mater. 2021, 4, 4575−4581

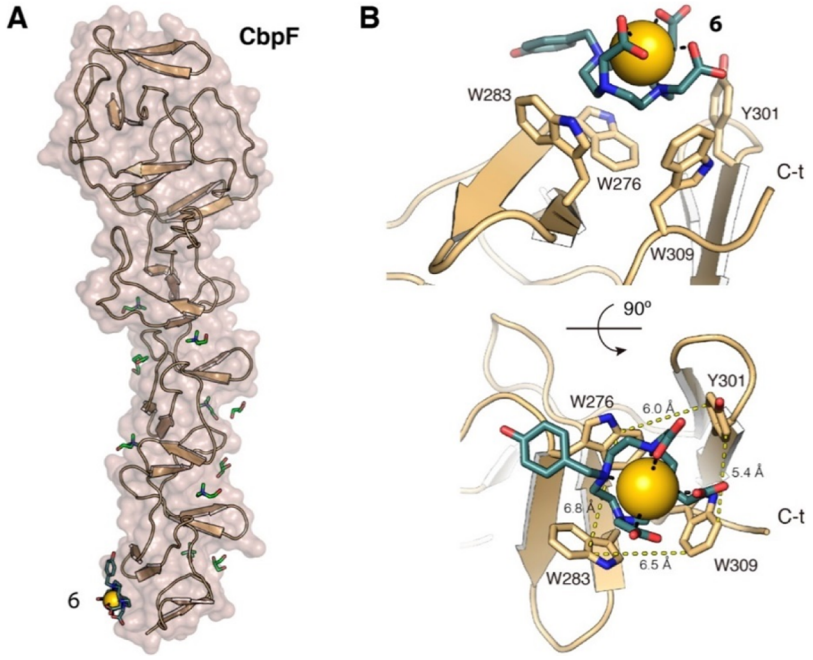

Figure 2. Cage complex **1** attachment to the CbpF protein surface. (A) 3D structure of CbpF represented by its molecular surface (colored in brown and with transparency) and by cartoon. Ligand **1** is presented as dark-green sticks. The remaining ligands bound to the CbpF surface are presented as light-green sticks. (B) Detailed view of ligand **1** (green sticks) bound to a choline-binding site of CbpF. Relevant residues are represented as capped sticks and labeled. The Yb atom is represented as a yellow sphere.

biomacromolecule crystallography; (2) using a tricarboxyl-based clathrochelating ligand to build up a neutral, Yb(III)-caged complex, which should be endowed with both the well-known chemical stability of the caged lanthanide complexes[39] and hydrophobicity sufficient to efficiently bind to common, accessible protein hydrophobic pockets (e.g., choline-binding sites), that is, without requiring occupancy or vacancy at the binding metal center to increase the efficiency of the binding to the protein; (3) involving a reactive peripheral functionalizing group to easily achieve further chemical modulation of the phasing agent,[38] if required, for example, to improve the solubility in the aqueous crystals of the mother liquor,[47] or for linking a fluorescent tag to discern marked versus unmarked crystals,[43] or a biorecognition moiety for specific protein (or other biomacromolecule) binding;[48] and (4) synthetic accessibility.

Taking into account all the above premises, we selected the neutral Yb(III)-based phasing agent **1** (Scheme 1), which is based on a previously reported, easily accessible clathrochelating ligand based on flexible tetraazacyclododecane with three pending carboxyl groups.[44,45]

Phasing Agent Validation. Once in hand, the capability of **1** to both bind biomacromolecules and to be used as a new agent for experimental phasing in large, complex molecules was analyzed. As a proof of principle, we chose the choline-binding protein F (CbpF) whose three-dimensional structure is known[33] and for which we have previously reported the binding modes of several caged Gd complexes.[34,36] This way, we could compare the binding properties of Gd versus Yb agents. The CbpF:**1** complex was obtained by fast soaking (~10 s) of native CbpF crystals into a mother liquor solution containing compound **1**. The excellent solubility of compound **1** in aqueous media allowed us to make the soaking at a high concentration of the ligand (25 mM) without damaging the CbpF crystal. Noticeably, compound **1** was able to efficiently decorate the model protein crystal with heavy atoms without further chemical modifications, also allowing its structural elucidation by efficient *de novo* phasing.

Structure of CbpF. Complex **1** was *de novo*-solved at 2.26 Å resolution using the XALOC beamline at the ALBA synchrotron (Barcelona, Spain). In order to test the phasing ability of **1** with conventional X-ray energies in macromolecular crystallography, the wavelength was kept at 0.97934 Å (12.659 keV), which corresponds to the maximum intensity of this beamline,[49] without performing any fluorescence scan to reach the wavelength corresponding to the Yb absorption edge. The data collected at ~1 Å, where the anomalous signal from the Yb(III) phasing agent is not expected to be high, were sufficient to drive the *de novo* structure solution by using only this anomalous signal. To the best of our knowledge, this is the first example where the weaker anomalous signal at 1 Å of a neutral Ln(III)-caged complex enables *de novo* structure determination of a large and unmodified biomacromolecule without setting the wavelength of the incident beam radiation near to that of the heavy-atom L_{III} absorption edge.

Although the concentrations of heavy atoms in protein crystals in the range of the ones used herein are expected to lead to increased radiation damage,[50] we did not observe such effect with our Yb(III) complex, as also observed with caged Gd complexes.[36] It has been presumed that the cage formed by the respective complex ligands might protect the protein from the effects of X-ray absorption by the heavy Ln atom.[36]

Noticeably, one single position for the Yb atom was localized in the anomalous difference map (Figure 1), with the occupancy of 1.0 using SHELXD.[51] SAD phasing was carried out using CRANCK2.[35] Experimental phases from this single Yb atom provided an excellent experimental electron-density map, permitting straightforward CbpF model building (Figure 1). Among the 311 residues comprising the full-length CbpF structure, 278 residues (90%) were automatically modeled by

https://doi.org/10.1021/acsabm.1c00305
ACS Appl. Bio Mater. 2021, 4, 4575−4581

auto-building using Buccaneer.[52] The remaining residues were manually included in the map by using Coot.[29] Besides the macromolecule, six choline molecules, three glycerol molecules, one PEG molecule, and one molecule of compound **1** were also identified and modeled bound to the CbpF molecular surface (Figure 2). The complete CbpF protein and ligands were refined, providing excellent statistics (Table 1). The compound **1** is found in one of the seven different choline-binding sites present in the CbpF structure composed of four aromatic residues (Trp276, Trp283, Tyr301, and Trp309) (Figure 1). These four residues create a large neutral cavity (Figure 1) in which the complex's tetraaza-macrocycle lies. Interestingly, the CbpF square-like cavity (Figure 2) accommodates the tetraaza-macrocycle by CH−π interactions (Figure 1), and no relevant polar interactions are detected between **1** and CbpF.

As designed, the clathrochelating ligand of **1** perfectly encases the Yb(III) center, providing hexa-coordination of the metallic cation by establishing polar interactions through the involved carboxylate moieties (i.e., forming a neutral complex with an average O−Yb distance of 3.0 Å) and by three out of the four nitrogen atoms of the tetraazacyclododecane moiety (average N−Yb distance of 2.4 Å) (Figure 3).

Table 1. Crystal Data and Structure Refinement Details for Compound 1[a]

CbpF:**1** complex	
Data Collection Statistics	
wavelength (Å)	0.97934
space group	$P2_12_12$
unit cell dimensions *a*, b, c (Å)	114.90, 52.20, 73.99
α, β, γ (deg)	90, 90, 90
resolution range (Å)	47.53−2.26 (2.33−2.26)
no. of unique reflections	21,487 (1930)
completeness (%)	98.8 (99.9)
multiplicity	7.8 (8.4)
CC1/2[b]	0.99 (0.75)
R_{pim}[c]	0.041 (0.97)
avg. $I/\sigma(I)$	6.3 (0.4)
Refinement Statistics	
resolution range (Å)	47.53−2.26
R_{work}/R_{free}[d]	0.21/0.24
no. of atoms	
protein	2580
water	44
ligand	103
RMS deviations	
bond length (Å)	0.003
bond angles (deg)	0.59
Ramachandran plot	
favored/outlier regions (%)	94.17/0.32
monomers per AU	1
PDB code	7BAY

[a]Values within parentheses correspond to the highest resolution shells. [b]CC1/2 is the correlation coefficient between intensity estimates from half data sets. [c]R_{pim} measures the precision of averaged intensities. $R_{pim} = \Sigma_{hkl}[1/(N-1)]1/2\Sigma_i|I_i(hkl) - [I(hkl)]|/\Sigma_{hkl}\Sigma_i I_i(hkl)$, where $\Sigma_i I_i(hkl)$ is the *i*th measurement of reflection *hkl*, $[I(hkl)]$ is the weighted mean of all measurements, and *N* is the redundancy for the *hkl* reflection. [d]$R_{work}/R_{free} = \Sigma_{hkl}|F_o - F_c|/\Sigma_{hkl}|F_o|$, where F_c is the calculated and F_o is the observed structure factor amplitude of reflection *hkl* for the working/free (5%) set, respectively. The atomic coordinates and structure factors for the CbpF:**1** complex (PDB 7BAY) have been deposited in the Protein Data Bank, Research Collaboratory for Structural Bioinformatics, Rutgers University, New Brunswick, New Jersey, USA (http://www.rcsb.org/).

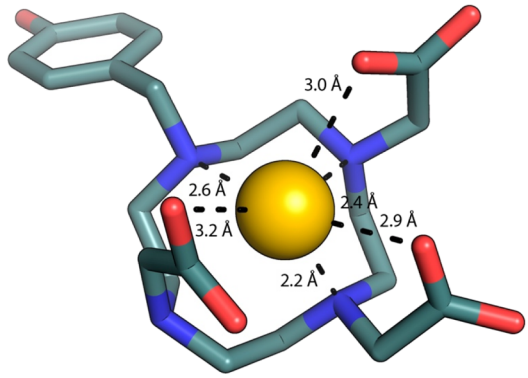

Figure 3. 3D structure of **1**. Molecular structure of **1** as observed in the CbpF:**1** complex at 2.26 Å resolution. The Yb atom (yellow sphere) is hexa-coordinated by three carboxylate oxygens (O−Yb distances, 2.9−3.2 Å) and three nitrogen atoms of the involved macrocycle (N−Yb distances, 2.2−2.6 Å). The fourth macrocycle nitrogen also interacts with the metal core but with a longer distance (N−Yb distance, 3.0 Å).

CONCLUSIONS

We demonstrate the first phasing agent based on a neutral Ln(III)-caged complex enabling *de novo* structure determination at 0.97934 Å of a 36 kDa native protein (311 residues) from human pathogen *Streptococcus pneumoniae* using the SAD method. The new powerful and versatile phasing agent assembled ytterbium(III), as the heavy Ln(III) center, and a tricarboxyl-based clathrochelating ligand, building up a neutral Yb(III)-caged complex capable of efficiently binding to common, accessible protein hydrophobic pockets by simple soaking. Interestingly, the no need for metal occupancy or vacancy to increase the agent's binding efficiency diminishes the probability of undesired structural distortions when decorating the crystal. Although this ytterbium-based phasing agent provides a strong anomalous signal at its L_{III} absorption edge, placed at 1.3863 Å, its expected weaker scatter signal at shorter wavelengths is suitable to drive *de novo* structure solution using only its anomalous signal without additional setting and/or previous sample modification. Crystallographic analysis shows the new agent to be nondisruptive for the diffraction quality of the heavy-metal-decorated protein crystals. The developed Yb(III) complex allows determining accurate phases, leading to high-quality experimental electron density maps that enabled the full tracing of the protein structure, with just one phasing agent unit bound to the macromolecule. The proof of principle reported here is the only successful phasing attempt in proving that the routinely collected high-resolution datasets from strongly diffracting crystals, using X-rays of shorter wavelengths (around 1.0 Å), can drive *de novo* 3D structure determination without demanding long-wavelength (1.5−2.5 Å) X-rays to maximize the accuracy and strength of the required anomalous signal. Therefore, the new Yb(III) complex becomes an effective phasing tool to overcome the important drawbacks imposed by the strategies currently applied to face this challenge, such as (1) biologically producing the heavy-atom-protein analogues

https://doi.org/10.1021/acsabm.1c00305
ACS Appl. Bio Mater. 2021, 4, 4575−4581

and/or (2) setting the incident beamline wavelength at the heavy-atom-absorption edge, far from the optimized synchrotron radiation wavelength, which drastically limits both the maximum resolution and the data quality through increased absorption, as well as radiation damage and harmonic contamination probability. Work in progress is devoted to further chemical modulation of Yb(III) complex derivatives to hasten them as advanced agents for solving native protein structures by *de novo* phasing.

AUTHOR INFORMATION

Corresponding Authors

María J. Ortiz − *Departamento de Química Orgánica, Facultad de Ciencias Químicas, Universidad Complutense de Madrid, 28040 Madrid, Spain;* orcid.org/0000-0002-0394-4045; Email: mjortiz@quim.ucm.es

Juan A. Hermoso − *Departamento de Cristalografía y Biología Estructural, Instituto de Química Física "Rocasolano", C.S.I.C., 28006 Madrid, Spain;* orcid.org/0000-0002-1862-8950; Email: xjuan@iqfr.csic.es

Authors

Alejandro Prieto-Castañeda − *Departamento de Química Orgánica, Facultad de Ciencias Químicas, Universidad Complutense de Madrid, 28040 Madrid, Spain*

Siseth Martínez-Caballero − *Departamento de Cristalografía y Biología Estructural, Instituto de Química Física "Rocasolano", C.S.I.C., 28006 Madrid, Spain*

Antonia R. Agarrabeitia − *Departamento de Química Orgánica, Facultad de Ciencias Químicas, Universidad Complutense de Madrid, 28040 Madrid, Spain*

Inmaculada García-Moreno − *Departamento de Sistemas de Baja Dimensionalidad, Superficies y Materia Condensada, Instituto de Química Física "Rocasolano", C.S.I.C., 28006 Madrid, Spain*

Santiago de la Moya − *Departamento de Química Orgánica, Facultad de Ciencias Químicas, Universidad Complutense de Madrid, 28040 Madrid, Spain;* orcid.org/0000-0002-7406-909X

Complete contact information is available at: https://pubs.acs.org/10.1021/acsabm.1c00305

Author Contributions

A. P.-C. and S. M.-C. contributed equally to this work.

Notes

The authors declare no competing financial interest.

ACKNOWLEDGMENTS

Financial support from Spanish Ministry of Science and Innovation (MAT2017-83856-C3-1 and C3-2, BFU2017-90030-P, PID2020-114755GB-C3 and PID2020-115331GB-I00 grants) is gratefully acknowledged. Technical support provided by staff at the ALBA Synchrotron facility (Barcelona, Spain) is also acknowledged. A.P.-C. thanks Consejería de Educación, Juventud y Deporte de la Comunidad de Madrid, and Fondo Social Europeo for a predoctoral contract (CT2/17/CT3/17/PEJ16/MED/AI-1598).

REFERENCES

(1) Garman, E.; Murray, J. W. Heavy-atom derivation. *Acta Crystallogr., Sect. D: Biol. Crystallogr.* **2003**, *59*, 1903−1913.

(2) Lu, J.; Sun, P. D. A Rapid and Rational Approach to Generating Isomorphous Heavy-atom Phasing Derivatives. *FEBS J.* **2014**, *281*, 4021−4028.

(3) Hendrickson, W. A.; Horton, J. R.; LeMaster, D. M. Selenomethionyl Proteins Produced for Analysis by Multiwavelength Anomalous Diffraction (MAD): a Vehicle for Direct Determination of Three-dimensional Structure. *EMBO J.* **1990**, *9*, 1665−1672.

(4) Doublié, S. Preparation of Selenomethionyl Proteins for Phase Determination. *Methods Enzymol.* **1997**, *276*, 523−530.

(5) Ribeiro, D.; Kulakova, A.; Quaresma, P.; Pereira, E.; Bonifácio, C.; Romão, M. J.; Franco, R.; Carvalho, A. L. Use of Gold Nanoparticles as Additives in Protein Crystallization. *Cryst. Growth Des.* **2014**, *14*, 222−227.

(6) Dauter, Z.; Dauter, M.; Rajashankar, K. R. Novel Approach to Phasing Proteins: Derivatization by Short Cryo-soaking with Halides. *Acta Crystallogr., Sect. D: Biol. Crystallogr.* **2000**, *56*, 232−237.

(7) Evans, G.; Bricogne, G. Triiodide Derivatization and Combinatorial Counter-ion Replacement: Two Methods for Enhancing Phasing Signal using Laboratory Cu *Kα* X-ray equipment. *Acta Crystallogr., Sect. D: Biol. Crystallogr.* **2002**, *58*, 976−991.

(8) Beck, T.; Krasauskas, A.; Gruene, T.; Sheldrick, G. M. A Magic Triangle for Experimental Phasing of Macromolecules. *Acta Crystallogr., Sect. D: Biol. Crystallogr.* **2008**, *64*, 1179−1182.

(9) Beck, T.; Gruene, T.; Sheldrick, G. M. The Magic Triangle Goes MAD: Experimental Phasing with a Bromine Derivative. *Acta Crystallogr., Sect. D: Biol. Crystallogr.* **2010**, *66*, 374−380.

(10) Abendroth, J.; Gardberg, A. S.; Robinson, J. I.; Christensen, J. S.; Staker, B. L.; Myler, P. J.; Stewart, L. J.; Edwards, T. E. SAD Phasing using Iodide Ions in a High-throughput Structural Genomics Environment. *J. Struct. Funct. Genomics* **2011**, *12*, 83−95.

(11) Boggon, T. J.; Shapiro, L. Screening for phasing atoms in protein crystallography. *Structure* **2000**, *8*, R143−R149.

(12) Agniswamy, J.; Joyce, M. G.; Hammer, C. H.; Sun, P. D. Towards a Rational Approach for Heavy-atom Derivative Screening in Protein Crystallography. *Acta Crystallogr., Sect. D: Biol. Crystallogr.* **2008**, *64*, 354−367.

(13) Joyce, M. G.; Radaev, S.; Sun, P. D. A Rational Approach to Heavy-atom Derivative Screening. *Acta Crystallogr., Sect. D: Biol. Crystallogr.* **2010**, *66*, 358−365.

(14) Knäblein, J.; Neuefeind, T.; Schneider, F.; Bergner, A.; Messerschmidt, A.; Löwe, J.; Steipe, B.; Huber, R. $Ta_6Br^2_{12}$, a Tool for Phase Determination of Large Biological Assemblies by X-ray Crystallography. *J. Mol. Biol.* **1997**, *270*, 1−7.

(15) Yonath, A.; Harms, J.; Hansen, H. A. S.; Bashan, A.; Schlünzen, F.; Levin, I.; Koelln, I.; Tocilj, A.; Agmon, I.; Peretz, M.; Bartels, H.; Bennett, W. S.; Krumbholz, S.; Janell, D.; Weinstein, S.; Auerbach, T.; Avila, H.; Piolleti, M.; Morlang, S.; Franceschi, F. Crystallographic Studies on the Ribosome, a Large Macromolecular Assembly Exhibiting Severe Nonisomorphism, Extreme Beam Sensitivity and No Internal Symmetry. *Acta Crystallogr., Sect. A: Found. Crystallogr* **1998**, *54*, 945−955.

(16) Cohen, A.; Ellis, P.; Kresge, N.; Soltis, S. M. MAD Phasing with Krypton. *Acta Crystallogr., Sect. D: Biol. Crystallogr.* **2001**, *57*, 233−238.

(17) Pike, A. C. W.; Garman, E. F.; Krojer, T.; von Delft, F.; Carpenter, E. P. An Overview of Heavy-atom Derivatization of Protein Crystals. *Acta Crystallogr., Sect. D: Struct. Biol.* **2016**, *72*, 303−318.

(18) Chaudhuri, B. N.; Sawaya, M. R.; Kim, C.-Y.; Waldo, G. S.; Park, M. S.; Terwilliger, T. C.; Yeates, T. O. The Crystal Structure of the First Enzyme in the Pantothenate Biosynthetic Pathway, Ketopantoate Hydroxymethyltransferase, from M. Tuberculosis. *Structure* **2003**, *11*, 753−764.

(19) de Bono, S.; Riechmann, L.; Girard, E.; Williams, R. L.; Winter, G. A Segment of Cold Shock Protein Directs the Folding of a Combinatorial Protein. *Proc. Natl. Acad. Sci. U.S.A.* **2005**, *102*, 1396−1401.

(20) Hermoso, J. A.; Lagartera, L.; González, A.; Stelter, M.; García, P.; Martínez-Ripoll, M.; García, J. L.; Menéndez, M. Insights into

Pneumococcal Pathogenesis from the Crystal Structure of the Modular Teichoic Acid Phosphorylcholine Esterase Pce. *Nat. Struct. Mol. Biol.* **2005**, *12*, 533−538.
(21) Jeudy, S.; Stelter, M.; Coutard, B.; Kahn, R.; Abergel, C. Preliminary Crystallographic Analysis of the Escherichia Coli YeaZ Protein using the Anomalous Signal of a Gadolinium Derivative. *Acta Crystallogr., Sect. F: Struct. Biol. Cryst. Commun.* **2005**, *61*, 848−851.
(22) Márquez, J.; Reinelt, S.; Koch, B.; Engelmann, R.; Hengstenberg, W.; Scheffzek, K. Structure of the Full-length Enzyme I of the Phosphoenolpyruvate-dependent Sugar Phosphotransferase System. *J. Biol. Chem.* **2006**, *281*, 32508−32515.
(23) Gras, S.; Chaumont, V.; Fernandez, B.; Carpentier, P.; Charrier-Savournin, F.; Schmitt, S.; Pineau, C.; Flament, D.; Hecker, A.; Forterre, P.; Armengaud, J.; Housset, D. Structural Insights into a New Homodimeric Self-activated GTPase Family. *EMBO Rep.* **2007**, *8*, 569−575.
(24) Molina, R.; González, A.; Stelter, M.; Pérez-Dorado, I.; Kahn, R.; Morales, M.; Campuzano, S.; Campillo, N. E.; Mobashery, S.; García, J. L.; García, P.; Hermoso, J. A.; Hermoso, J. A. Crystal Structure of CbpF, a Bifunctional Choline-binding Protein and Autolysis Regulator from Streptococcus Pneumoniae. *EMBO Rep.* **2009**, *10*, 246−251.
(25) Arnoux, P.; Morosinotto, T.; Saga, G.; Bassi, R.; Pignol, D. A Structural Basis for the pH-Dependent Xanthophyll Cycle in Arabidopsis thaliana. *Plant Cell* **2009**, *21*, 2036−2044.
(26) Pérez-Dorado, I.; González, A.; Morales, M.; Sanles, R.; Striker, W.; Vollmer, W.; Mobashery, S.; García, J. L.; Martínez-Ripoll, M.; García, P.; Hermoso, J. A. Insights into Pneumococcal Fratricide from the Crystal Structures of the Modular Killing Factor LytC. *Nat. Struct. Mol. Biol.* **2010**, *17*, 576−581.
(27) Pérez-Dorado, I.; Sanles, R.; González, A.; García, P.; García, J. L.; Martínez-Ripoll, M.; Hermoso, J. A. Crystallization of the Pneumococcal Autolysin LytC: In-house Phasing using Novel Lanthanide Complexes. *Acta Crystallogr., Sect. F: Struct. Biol. Cryst. Commun.* **2010**, *66*, 448−451.
(28) Girard, É.; Stelter, M.; Vicat, J.; Kahn, R. A New Class of Lanthanide Complexes to Obtain High-phasing-power Heavy-atom Derivatives for Macromolecular Crystallography. *Acta Crystallogr., Sect. D: Biol. Crystallogr.* **2003**, *59*, 1914−1922.
(29) Emsley, P.; Lohkamp, B.; Scott, W. G.; Cowtan, K. Features and Development of Coot. *Acta Crystallogr., Sect. D: Biol. Crystallogr.* **2010**, *66*, 486−501.
(30) Evans, P. R.; Murshudov, G. N. How Good Are My Data and What Is the Resolution? *Acta Crystallogr., Sect. D: Biol. Crystallogr.* **2013**, *69*, 1204−1214.
(31) Kabsch, W. XDS. *Acta Crystallogr., Sect. D: Biol. Crystallogr.* **2010**, *66*, 125−132.
(32) Liu, Q.; Hendrickson, W. A. Crystallographic Phasing from Weak Anomalous Signals. *Curr. Opin. Struct. Biol.* **2015**, *34*, 99−107.
(33) Molina, R.; González, A.; Moscoso, M.; García, P.; Stelter, M.; Kahn, R.; Hermoso, J. A. Crystallization and Preliminary X-ray Diffraction Studies of Choline-binding Protein F from Streptococcus Pneumoniae. *Acta Crystallogr., Sect. F: Struct. Biol. Cryst. Commun.* **2007**, *63*, 742−745.
(34) Molina, R.; Stelter, M.; Kahn, R.; Hermoso, J. A. Characterization of Gadolinium Complexes for SAD Phasing in Macromolecular Crystallography: Application to CbpF. *Acta Crystallogr., Sect. D: Biol. Crystallogr.* **2009**, *65*, 823−831.
(35) Skubák, P.; Pannu, N. S. Automatic Protein Structure Solution from Weak X-ray Data. *Nat. Commun.* **2013**, *4*, 2777.
(36) Stelter, M.; Molina, R.; Jeudy, S.; Kahn, R.; Abergel, C.; Hermoso, J. A. A Complement to the Modern Crystallographer's Toolbox: Caged Gadolinium Complexes with Versatile Binding Modes. *Acta Crystallogr., Sect. D: Biol. Crystallogr.* **2014**, *70*, 1506−1516.
(37) Vagin, A.; Teplyakov, A. Molecular Replacement with MOLREP. *Acta Crystallogr., Sect. D: Biol. Crystallogr.* **2010**, *66*, 22−25.
(38) Zelinskii, G. E.; Belov, A. S.; Belaya, I. G.; Vologzhanina, A. V.; Novikov, V. V.; Varzatskii, O. A.; Voloshin, Y. Z. The Molecular Design of Cage Metal Complexes for Biological Applications: Pathways of the Synthesis, and X-ray Structures of a Series of New N_2-, S_2- and O_2-alicyclic Iron(II) di- and tetrachloroclathrochelates. *New J. Chem.* **2018**, *42*, 56−66.
(39) Girard, É.; Anelli, P. L.; Vicat, J.; Kahn, R. High-phasing-power Lanthanide Derivatives: Taking Advantage of Ytterbium and Lutetium for Optimized Anomalous Diffraction Experiments using Synchrotron Radiation. *Acta Crystallogr., Sect. D: Biol. Crystallogr.* **2003**, *59*, 1877−1880.
(40) Girard, É.; Chantalat, L.; Vicat, J.; Kahn, R. Gd-HPDO3A, a Complex To Obtain High-phasing-power Heavy-atom Derivatives for SAD and MAD Experiments: Results with Tetragonal Hen Egg-white Lysozyme. *Acta Crystallogr., Sect. D: Biol. Crystallogr.* **2002**, *58*, 1−9.
(41) Barends, T. R. M.; Foucar, L.; Botha, S.; Doak, R. B.; Shoeman, R. L.; Nass, K.; Koglin, J. E.; Williams, G. J.; Boutet, S.; Messerschmidt, M.; Schlichting, I. De Novo Protein Crystal Structure Determination from X-ray Free-electron Laser Data. *Nature* **2014**, *505*, 244−247.
(42) Doutch, J.; Hough, M. A.; Hasnain, S. S.; Strange, R. W. Challenges of Sulfur SAD Phasing as a Routine Method in Macromolecular Crystallography. *J. Synchrotron Radiat.* **2012**, *19*, 19−29.
(43) Engilberge, S.; Riobé, F.; Di Pietro, S.; Lassalle, L.; Coquelle, N.; Arnaud, C.-A.; Pitrat, D.; Mulatier, J.-C.; Madern, D.; Breyton, C.; Maury, O.; Girard, E. Crystallophore: a Versatile Lanthanide Complex for Protein Crystallography Combining Nucleating Effects, Phasing Properties, and Luminescence. *Chem. Sci.* **2017**, *8*, 5909−5917.
(44) Karhunen, U.; Rosenberg, J.; Lamminmäki, U.; Soukka, T. Homogeneous Detection of Avidin Based on Switchable Lanthanide Luminescence. *Anal. Chem.* **2011**, *83*, 9011−9016.
(45) Lippert, A. R.; Gschneidtner, T.; Chang, C. J. Lanthanide-based Luminescent Probes for Selective Time-gated Detection of Hydrogen Peroxide in Water and in Living Cells. *Chem. Commun.* **2010**, *46*, 7510−7512.
(46) Afonine, P. V.; Grosse-Kunstleve, R. W.; Echols, N.; Headd, J. J.; Moriarty, N. W.; Mustyakimov, M.; Terwilliger, T. C.; Urzhumtsev, A.; Zwart, P. H.; Adams, P. D. Towards Automated Crystallographic Structure Refinement with Phenix.refine. *Acta Crystallogr., Sect. D: Biol. Crystallogr.* **2012**, *68*, 352−367.
(47) Zhang, T.; Zhu, X.; Cheng, C. C. W.; Kwok, W.-M.; Tam, H.-L.; Hao, J.; Kwong, D. W. J.; Wong, W.-K.; Wong, K.-L. Water-Soluble Mitochondria-Specific Ytterbium Complex with Impressive NIR Emission. *J. Am. Chem. Soc.* **2011**, *133*, 20120−20122.
(48) Wu, X.; Li, L.; Shi, W.; Gong, Q.; Ma, H. Near-Infrared Fluorescent Probe with New Recognition Moiety for Specific Detection of Tyrosinase Activity: Design, Synthesis, and Application in Living Cells and Zebrafish. *Angew. Chem., Int. Ed.* **2016**, *55*, 14728−14732.
(49) Juanhuix, J.; Gil-Ortiz, F.; Cuní, G.; Colldelram, C.; Nicolás, J.; Lidón, J.; Boter, E.; Ruget, C.; Ferrer, S.; Benach, J. Developments in Optics and Performance at BL13-XALOC, the Macromolecular Crystallography Beamline at the Alba Synchrotron. *J. Synchrotron Radiat.* **2014**, *21*, 679−689.
(50) Coughlan, H. D.; Darmanin, C.; Phillips, N. W.; Hofmann, F.; Clark, J. N.; Harder, R. J.; Vine, D. J.; Abbey, B. Radiation Damage in a Micron-sized Protein Crystal Studied via Reciprocal Space Mapping and Bragg Coherent Diffractive Imaging. *Struct. Dyn.* **2015**, *2*, 041704.
(51) Sheldrick, G. M. Experimental Phasing with SHELXC/D/E: Combining Chain Tracing with Density Modification. *Acta Crystallogr., Sect. D: Biol. Crystallogr.* **2010**, *66*, 479−485.
(52) Cowtan, K. The Buccaneer Software for Automated Model Building. 1. Tracing Protein Chains. *Acta Crystallogr., Sect. D: Biol. Crystallogr.* **2006**, *62*, 1002−1011.

https://doi.org/10.1021/acsabm.1c00305
ACS Appl. Bio Mater. 2021, 4, 4575−4581